Improvement in secondary cooling of continuous casting of round billets through analysis of heat flux distribution

C. Assuncao*, R. Tavares and G. Oliveira

A mathematical model of heat transfer and solidification for a continuous casting of round billets was developed. The water flux density of the secondary cooling zone was experimentally measured, using an apparatus in industrial scale with two types of nozzles, flat jet and full cone jet. The profiles of water distribution were applied on the mathematical model. The results showed that the water distribution is not uniform in both longitudinal and angular directions owing to the unevenness of the spray and to the curvature effect of the round billet. This non-uniformity causes important variation of the heat transfer coefficients and superficial temperature of the billet, especially in the first cooling zones, where the temperature is higher. The mathematical model was used to simulate a change of nozzle type in the first cooling zone. The results showed that the heat flux and superficial temperature variations were reduced with a full cone jet nozzle in comparison with the flat jet nozzles.

Keywords: Water flux distribution, Heat transfer coefficient, Secondary cooling, Round billet, Mathematical model

Introduction

The quality of the steel in the continuous casting is directly related to the temperature variation during the solidification process.[1] Inappropriate temperature profiles can cause defects such as cracks, deep oscillation marks, depressions, inclusions and geometric deviation.[2] The knowledge of the thermal behaviour of the steel is mandatory to define the best operational practices and, consequently, to reduce quality issues. In the mould, the superficial heat flux of the steel can be calculated relating the residence time inside the mould and the average heat flux.[3–8] An alternative approach that has been largely applied[9–12] is to use the inverse problem of heat conduction through the mould wall. In the secondary cooling zone, the superficial heat flux of steel involves different mechanisms, such as radiation in the dry zones, conduction in the regions in contact with the rolls and convection owing to the water sprays.[13] The heat extraction in the spray zone depends on the water pressure, stand-off distance between the strand and the nozzle, nozzle type, strand surface temperature and water flux. Exhaustive studies have been developed to identify the effect of these parameters of spray on the heat flux.[14,15] All the studies agree that, in the temperature range of interest, the water flux has the largest effect on the heat transfer coefficient. Since the water flux density varies locally along the secondary cooling zone, the heat flux and heat transfer coefficient vary locally as well. However, several authors assume a uniform water flux distribution in the heat transfer modelling. This assumption can lead to imprecision, especially in the evaluation of local phenomena. Some authors have measured the water flux density for different types of nozzles[16,17] for slabs and square billets, and the common conclusion is that the water flux distribution is not uniform. Despite this conclusion, the results of the non-uniformity have not been largely used in the heat transfer modelling.[18–20] Besides that, no reference of water flux density for round billets has been found in the literature. The present work was developed considering a continuous casting machine of round billets that has been facing to some quality problems, such as subsurface and mid radial cracks and internal overlapping in the following tube mill process. These defects have been attributed to the non-uniformity of the heat transfer of the billet in the secondary cooling. Therefore, the objectives of the present work are to determine experimentally the water flux density distribution of flat jet and full cone jet nozzles along the secondary cooling zone, to develop a mathematical model of heat transfer and solidification of steel, to investigate the effect of the non-uniformity of the water distribution on heat transfer coefficients (HTCs) and billet temperatures and to simulate the change of nozzle type.

Description of machine

The present work was developed considering a continuous casting machine of round billets. This machine has four strands and is capable of producing billets of 180 and 230 mm of diameters. The primary cooling of the steel takes place in the mould and the secondary cooling takes place in the spray chamber, which has four control

Department of Metallurgical and Materials Engineering, Universidade Federal de Minas Gerais, Belo Horizonte, Minas Gerais, Brazil

*Corresponding author, email charles.assuncao@vallourec.com

Published by Maney on behalf of the Institute
Received 26 February 2014; accepted 26 March 2014
DOI 10.1179/1743281214Y.0000000190

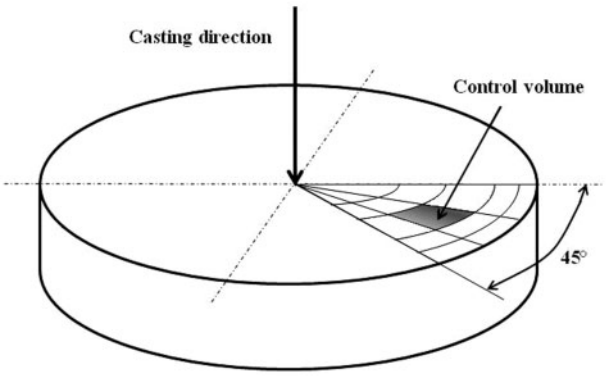

1 Control volume of slice of steel

zones (0, A, B and C). Zone 0 has two spray rings with eight nozzles each and another spray ring with four nozzles. These nozzles have a flat jet profile. In zones A–C, each spray ring has four nozzles at 90° from one another. These nozzles have a full cone jet profile. After the spray chamber, the round billet is straightened and cut in different lengths.

Mathematical model

The mathematical model of heat transfer and solidification of the billet has been developed taking into account the heat transfer by conduction in both radial and angular directions. The main assumptions are listed below:

(i) symmetry of transversal section, only one-eighth of the transversal section was modelled, as shown in Fig. 1
(ii) the heat transfer by conduction in the casting direction was neglected owing to the high Peclet number
(iii) the latent heat of steel solidification was converted into an equivalent specific heat capacity in the mushy zone
(iv) the density of the steel was considered constant, whereas the heat capacity, thermal conductivity and emissivity were temperature dependent
(v) the effects of strand shrinkage were neglected
(vi) the convective heat flow in the liquid pool and mushy zone was accounted for the effective thermal conductivity.[7]

The strand was divided into several slices of steel that move downwards in the casting direction at the casting speed. The domain of the model was divided in 400 control volumes where the energy balance was applied on, with 40 divisions in the radial direction and 10 divisions in the angular direction. The time interval of calculation Δt was 0·01 s.

The energy balance was obtained from the general energy conservation equation for cylindrical coordinates. In order to obtain the numerical solution, equation (1) was discretised and explicitly solved by finite volume method[21]

$$\rho\frac{\partial\left(C_p^{eq}T\right)}{\partial t}=\frac{1}{r}\frac{\partial}{\partial r}\left(rk_{ef}\frac{\partial T}{\partial r}\right)+S \quad (1)$$

where ρ is the density of steel (kg m^{-3}), C_p^{eq} is the equivalent heat capacity of steel (J kg^{-1} K^{-1}), r is the radial position of the control volume (m), k_{ef} is the effective thermal conductivity of steel (W m^{-1} K^{-1}), T is the temperature of steel (K), t is time (s) and S is the source term used to consider the boundary conditions (W m^{-3}).

The solidification was considered under equilibrium conditions, and the liquid fraction of the steel was determined by means of the lever rule equation,[22] according to equations (2) and (3)

$$f_{liq}=\frac{(T_0-T_L)-k(T_0-T)}{(1-k)(T_0-T)} \quad (2)$$

$$k=\frac{T_0-T_L}{T_0-T_S} \quad (3)$$

where T_0 is the melting temperature of pure iron (K), T_L is the liquidus temperature of the steel (K), T is the temperature of steel (K) and k is the partition coefficient.

The equivalent heat capacity of steel in mushy zone was calculated considering the effect of latent heat of steel solidification

$$C_P^{eq}=C_P+L\frac{dF}{dT} \quad (4)$$

$$\frac{dF}{dT}=\frac{(T_0-T_L)}{(1-k)(T_0-T)^2} \quad (5)$$

where C_P is heat capacity of solid steel (J kg^{-1} K^{-1}), and L is the latent heat of steel solidification (J kg^{-1}).

The convective effects in the liquid portion of steel were considered using an effective thermal conductivity

$$k_{ef}=k_{sol}\left[1+(C-1)f_l^2\right] \quad (6)$$

where f_l is the liquid fraction of steel in the mushy zone, C is a constant equal to 6 and k_{sol} is the thermal conductivity of the solid steel calculated by the equation of the Table 1.

Boundary conditions

The initial condition is $T_{steel}=T_{tundish}$, i.e. the temperature of steel is the same as that measured in the tundish.

Table 1 Physical properties of steel

Parameter	Value
Density[25]/kg m^{-3}	7020
Latent heat of solidification[25]/J kg^{-1}	272 000
Solidus temperature[26]/K	1809–415·5%C + 12·3%Si + 6·8%Mn + 124·5%P + 183·9%S + 4·1%Al
Liquidus temperature[26]/K	1809–78%C + 7·6%Si + 4·9%Mn + 34·4%P + 38%S + 3·6%Al
Specific heat[27]/J kg^{-1}	C_P=481·482 + 0·1997T_{steel} T_{steel}/°C
Thermal conductivity[28]/W m^{-1} K^{-1}	k_{sol}=15·9106 + 0·1151T_{steel} T_{steel}/°C
Emissivity[29]	ε=0·0002T_{steel} + 0·6274

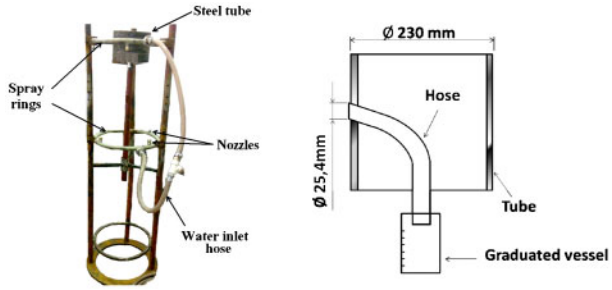

2 Set of water flux density measurement

In the mould, the boundary condition was expressed in terms of an average heat flux (MW m^{-2}),[23] as shown by equation (7)

$$q_{\text{mould}} = \alpha\left[2{\cdot}679 - 0{\cdot}221(t_{\text{mould}})^{1/2}\right] \quad (7)$$

where t_{mould} is the residence time of each slice of steel inside the mould, and α is the calibration factor for each cooling zone.

In the secondary cooling, the heat flux (W m^{-2}) was calculated by the following equations[24]

$$q_{\text{spray}} = h_{\text{g}}(T_{\text{steel}} - T_{\text{water}}) \quad (8)$$

$$h_{\text{g}} = h_{\text{conv}} + \sigma\varepsilon(T_{\text{steel}} + T_{\infty})\left(T_{\text{steel}}^2 + T_{\infty}^2\right) \quad (9)$$

$$h_{\text{conv}} = \alpha(708\,W^{0{\cdot}75}T^{-1{\cdot}2} + 0{\cdot}116) \quad (10)$$

where h_{g} is the global HTC (W m^{-2} K^{-1}), T_{steel} is the superficial temperature of steel (K), T_{water} is the temperature of the water spray (K), h_{conv} is the convection HTC (W m^{-2} K^{-1}), T_{∞} is the environment temperature (K) and W is the water flux density (L s^{-1} m^{-2}).

The calibration factors α were used to adjust the equations of the mould heat flux and the convection HTC obtained in the literature to the plant data, i.e. the average heat flux in the mould, estimated based on the water flowrate and temperature variation, and the superficial temperature in the secondary cooling zone.

Physical properties of steel

The physical properties of the steel considered in the model are shown in Table 1.

Experimental

The experimental procedures described in this section were performed to obtain the water flux density distribution at several positions along the secondary cooling zones.

Figure 2 shows the apparatus that was used to measure the water flux density distribution in zones 0, A, B and C. The apparatus had the same size and curvature of an actual strand. The spray rings were connected to a flexible hose of the system that supplied water to the nozzles. The nozzles used in the experiments were of the same type of those used in the actual plant. A small steel tube of outer diameter of 230 mm with a hole of 1 in of diameter in the wall was positioned at several locations in the impingement area of the water spray. In order to collect the impinging water, a hose was connected to the hole and conducted the water to a graduated container, as shown in Fig. 2. The system that supplied water to the nozzles consisted of a centrifugal pump of 0·75 kW, a control valve and a flow meter.

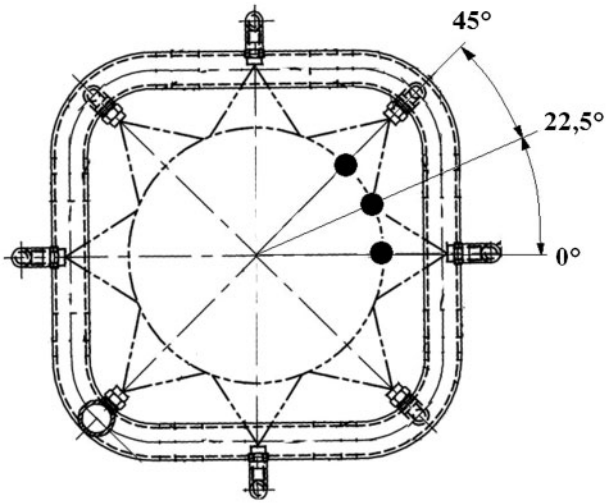

3 Scheme of zone 0 positioning

In the experiments corresponding to zone 0, nozzles 1/4 U-5010 (Spraying Systems) were used. The tube was centred in the spray ring in the same way the billet is in the plant. The distance between the collecting hole and the nozzles was 45 mm. The tube was placed at three different angular positions, as shown in Fig. 3. In the longitudinal direction, the tube was kept at the same position because the water impingement area of the flat nozzles is very thin. The water flowrate varied as shown in Table 2, and the gauge pressure was kept in 0·25 MPa, nozzles 1/4 GGA-3·9 (Spraying Systems) were used for zones A–C. This kind of nozzle has a full cone spray with a circular impingement area. Symmetries in both vertical and horizontal axes were assumed, and then the measurements were performed in a quarter of the water impingement area. The hole was placed at five different positions in the longitudinal direction and at three positions in the angular direction, as shown in Fig. 4. The distance between the hole and the spray ring was 115 mm, which is the same distance between the billet and the spray ring in the plant. The water flowrate varied as shown in Table 3, and the gauge pressure was kept in 0·29 MPa.

The local water flux density was calculated based on five measurements performed at each position and for each water flowrate.

Table 2 Water flowrate variation in zone 0

Number of experiment	1	2	3	4	5	6
Experimental water flowrate/L min^{-1}	7·0	9·0	11·0	13·0	16·0	18·0
Corresponding water flowrate*/L min^{-1}	47	60	73	87	107	120

*Calculated based on the number of nozzles of the cooling zone.

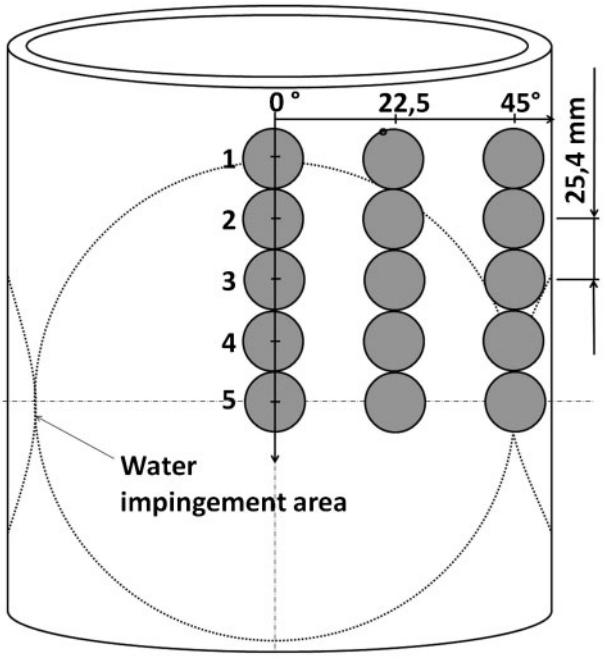

4 Positions of hole to measure water flux density

Results and discussion

Water distribution

The experimental water flux density at each position was calculated by equation (11)

$$WD_{\text{exp}} = \frac{V_{\text{water}}}{tA_{\text{h}}} \tag{11}$$

where WD_{exp} is the experimental water flux density (L s^{-1} m^{-2}), V_{water} is the volume of water collected in the graduated container (L), t is the time spent collecting the respective volume (s) and A_{h} is the area of the collecting hole (m^2).

Since the local water flux density was measured for different water flowrates, an index of water flux density was defined, according to equation (12), to enable the analysis of water distribution for different situations

$$I_{\text{WD}} = \frac{\sum_{\text{i}=1}^{\text{i}=\text{n}} \left(WD_{\text{exp}}/W_{\text{ring}}\right)_{\text{i}}}{n} \tag{12}$$

where I_{WD} is the index of water flux density (m^{-2}), W_{ring} is the water flowrate of the spray ring during each measurement (L s^{-1}), i identifies the number of the measurement and n is the total number of measurements. Thus, the local water flux density was calculated multiplying the index of water flux density by the water flowrate of each cooling zone.

Figure 5 shows the index of water flux density of zone 0 for eight nozzle condition (spray rings 1 and 2) and four nozzle condition (spray ring 3). The results for the eight nozzle condition at the angle 22·5° were not computed owing to experimental issues.

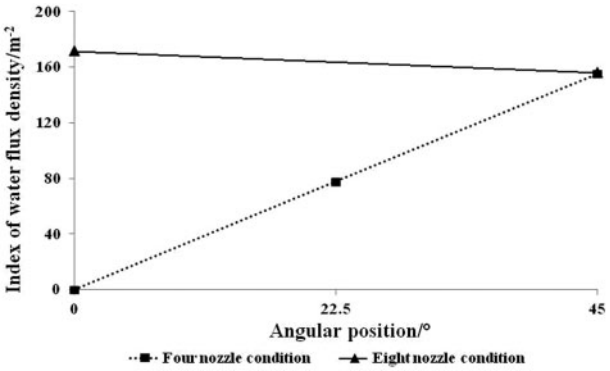

5 Index of water flux density of zone 0

The index of water flux density has a small variation in the angular direction for the eight nozzle condition, making the water distribution almost uniform for the first two spray rings. The index of water flux density varies considerably for the four nozzle condition. This difference is owing to the lack of a nozzle at the angle of 0° in the third spray ring.

Figure 6 shows the index of water flux density inside the water impingement area of the spray rings of the zones A–C.

The water distribution is not uniform in both longitudinal and angular directions. In the longitudinal direction for any angular position, the index of water flux density increases from the outer to the inner positions. It reaches its maximum value at the intermediate position, and it decreases as the position gets closer to the centre of the water impingement area. This profile agrees with that obtained elsewhere[30] and confirms that the full cone nozzles do not have an even water spray.

The index of water flux density varies considerably in the angular direction also because of the curvature of the tube. The higher is the angle, the smaller is the normal area of the collecting hole 'viewed' by the nozzle and then less water would impinge and be collected, as schematically shown in Fig. 7.

Besides the non-uniformity of the water spray of the nozzles, the water sprays do not cover all the surface of the strand, and there are several dry areas where the cooling is owing to natural convection and radiation mainly.

Figure 8 shows the water flux density along the cooling zones considering both uniform water distribution, which uses the average water flux density,[31] and non-uniform water distribution, which considers the experimental water flux density. Although the total amount of water is the same, the water distribution profiles are totally different.

Table 3 Water flowrates in zone 0

Number of experiment	1	2	3	4	5	6
Experimental water flowrate/L min^{-1}	3·0	3·5	4·1	4·7	5·3	5·9
Corresponding water flowrate zone A*/L min^{-1}	54	63	74	85	95	106
Corresponding water flowrate zone B*/L min^{-1}	42	49	57	66	74	83
Corresponding water flowrate zone C*/L min^{-1}	36	42	49	56	64	71

*Calculated based on the number of nozzles of the cooling zone.

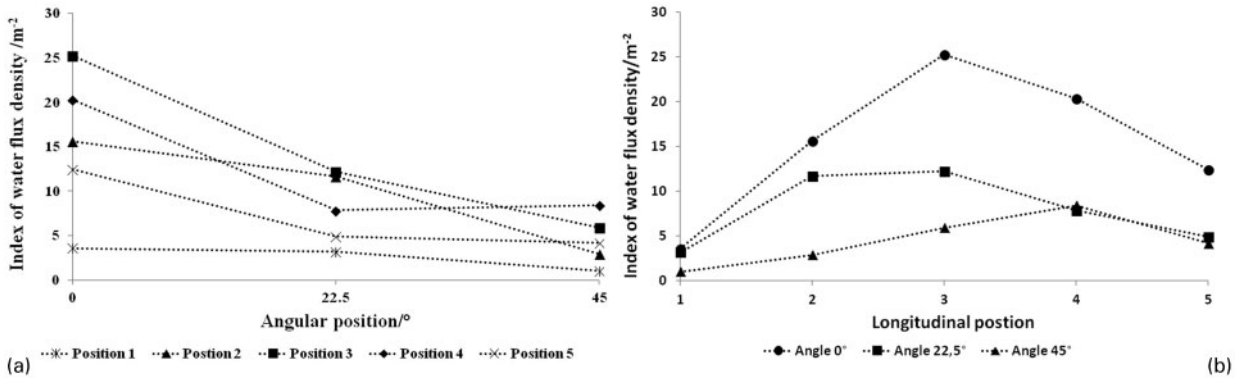

6 Index of water density for zones A–C

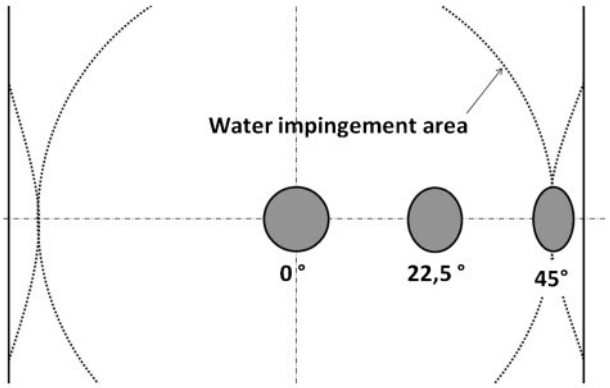

7 Effect of curvature of tube

Mathematical model

The results of water distribution were applied in the mathematical model of heat transfer and solidification of the round billets. The calibration factors and the casting conditions during the four temperature measurements are shown in Tables 4 and 5 respectively.

Figure 9 shows the superficial temperature profiles at the angles 0 and 45° and the shell thickness obtained by the mathematical model for a casting speed of 1·12 m min^{-1}. A good agreement between the measured and the calculated values of temperature was obtained. The differences of temperature in the angular direction are observed from the third spray ring of zone 0. The solidification profile is similar to those found in the literature.[19,20]

Figure 10 shows the profile of the global HTC in longitudinal direction at angle 0°

The non-uniformity of water density has an important effect on the global HTC, since the local water flux density is the main factor that affects the heat transfer by convection.[17] The highest variation of the global HTC occurs in the cooling zone 0. The peak values are ~6500 W m^{-2} K^{-1}, whereas the lowest values are ~220 W m^{-2} K^{-1}. If a uniform water density was considered, the global HTC would be ~500 W m^{-2} K^{-1} along the whole zone. In zones A–C, the global HTC varies from 200 W m^{-2} K^{-1}, at the dry areas, up to 500 W m^{-2} K^{-1}, at the wet areas.

As the global HTC varies more intensely in zone 0, the analysis was focused on this zone. The results of the water distribution experiments showed that the flat nozzles produce a concentrated jet in a very small area, generating an uneven cooling in zone 0. In order to reduce the cooling non-uniformity, the use of the full cone nozzles instead of the flat jet nozzles in zone 0 was simulated by the mathematical model.

Figure 11 shows the global HTC distribution with both flat jet nozzles and full cone jet nozzles obtained by the mathematical model with the same water flowrate. The variation of the global HTC with the full cone jet nozzles is smoother than with the flat jet nozzles since the full cone nozzle has a less concentrated jet and greater water impingement area. The heat flux is more uniform in both angular and longitudinal directions with the full cone jet nozzles.

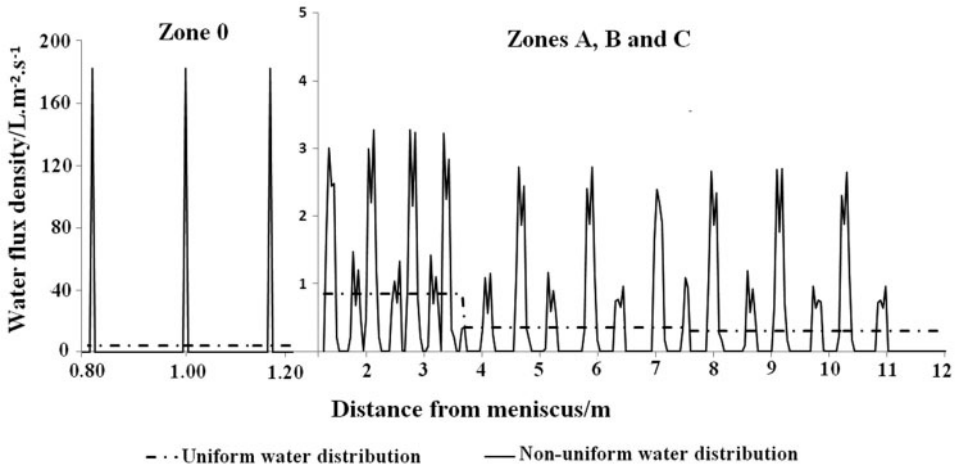

8 Water density distribution

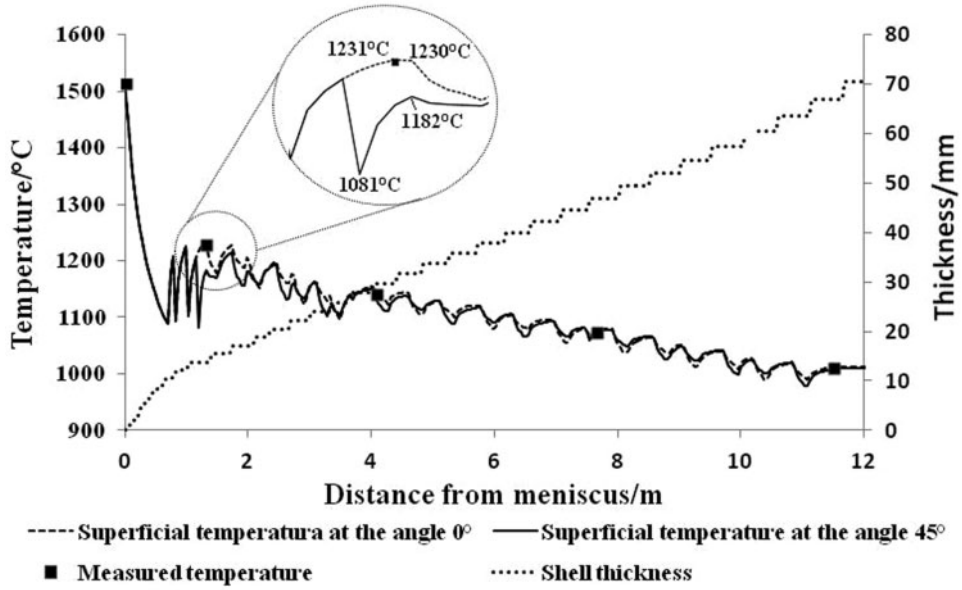

9 Results of superficial temperature and shell thickness variations

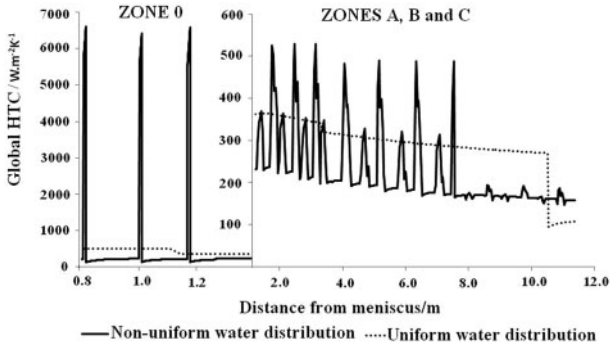

10 Global HTC variation in longitudinal direction

Figure 12 shows the temperature profiles in the longitudinal and angular directions in zone 0. With the flat jet nozzles, the temperature varies intensely in the longitudinal direction, right after the three spray rings, and in the angular direction at the third spray ring, with temperature variations larger than 230°C. With the full cone jet nozzles, the temperature variation reduces significantly in both directions as a consequence of the more even water flux and heat flux distributions. In this simulated condition, the temperature variation in both longitudinal and angular directions is under the acceptable limit of 100°C.[32]

Under the current conditions, the billet could be overcooled or reheated very intensely and in different ways at the same transversal section as it passes through the zones, especially in zone 0. This non-uniform cooling causes severe superficial thermal gradients, which can generate process deviations as expansion of billet surface, tensile stresses and strains at solidification front, compressive stresses on the surface and tensions on billet surface. These process deviations could result in longitudinal internal cracks, miradial cracks, and longitudinal depressions with subsurface longitudinal facial cracks.[18] The change of nozzle type was simulated and the results showed significant reduction in the variation of heat flux and superficial temperature.

Table 4 Calibration factor for each cooling zone

	Mould	Zone 0	Zone A	Zone B	Zone C
Calibration factor α	0·77	3·0	1·1	0·6	0·7

Conclusions

A mathematical model of the heat transfer and solidification for a continuous casting of round billet was developed and calibrated with superficial temperature

Table 5 Operational parameters during the temperature measurements

Parameter	1	2	3	4
Steel grade	4133	4133	E355	E355
Diameter of the round billet/mm	230	230	180	180
Casting speed/m min^{-1}	0·79	1·12	1·73	2·03
Tundish temperature/°C	1557	1514	1537	1532
Temperature at z=1·30 m °C^{-1}	1236	1228	1186	1217
Temperature at z=4·07 m °C^{-1}	1122	1142	1187	1189
Temperature at z=7·65 m °C^{-1}	…	1073	1133	1136
Temperature at z=11·50 m °C^{-1}	1013	1010	1108	1139
Water flowrate in mould/L min^{-1}	1948	1953	1936	1934
Water flowrate in zone 0/L min^{-1}	39	54·5	101	118
Water flowrate in zone A/L min^{-1}	40	53·5	84	98
Water flowrate in zone B/L min^{-1}	39	54·6	51	60
Water flowrate in zone C/L min^{-1}	23	33	51	60

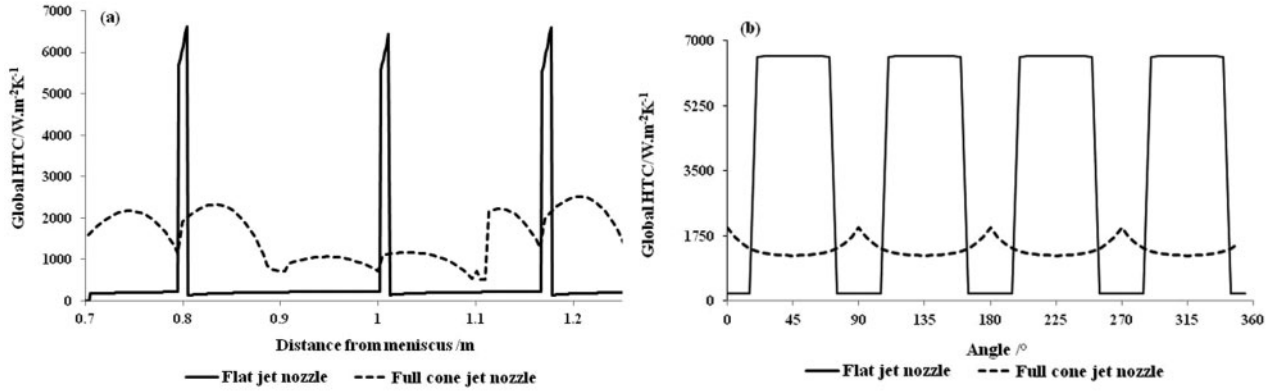

a longitudinal direction; *b* angular direction at third spray ring

11 Profile of global HTC

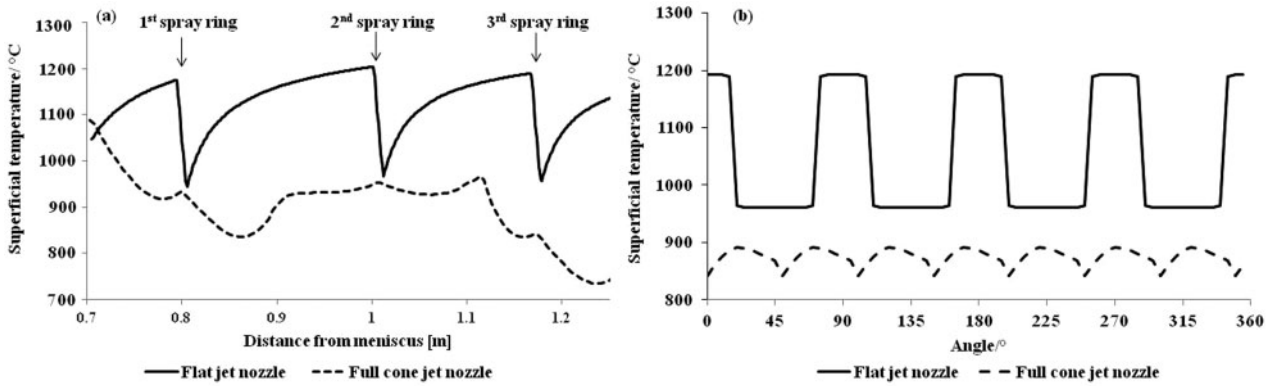

a longitudinal direction; *b* angular direction

12 Superficial temperature variation in zone 0

measurements in an industrial plant. Experimental measurements of water distribution in the secondary cooling zone were performed using flat jet and full cone jet nozzles. An index of water flux density that relates the water distribution with the total amount of water was defined and applied on the mathematical model. The experiments showed that the water distribution is not uniform in both angular and longitudinal directions for both types of nozzles. The mathematical model was used to investigate the effect of the non-uniformity of water distribution on heat transfer coefficients and billet superficial temperature and to simulate the change of nozzle type. The non-uniformity of the water distribution causes important variations in the heat transfer coefficients and superficial temperatures in both longitudinal and angular directions, especially in cooling zone 0. The simulations showed that the use of full cone nozzle instead of the flat jet nozzle would reduce the heat flux and superficial temperature variation, which could contribute to the reduction of quality issues.

This non-uniform water distribution approach is a useful tool to enhance the comprehension about the thermal behaviour of the steel along the secondary cooling in the continuous casting of round billets and to optimize the caster parameters to improve the quality of the as-cast product.

Acknowledgements

The financial support of Fundação de Amparo à Pesquisa do Estado de Minas Gerais (FAPEMIG), Brazil, in the form of a research grant to R. Tavares, process no. TEC-APQ-00373-11, is gratefully acknowledged. The authors also acknowledge the financial support of CAPES to the graduate program.

References

1. A. S. Sabau: 'Measurement of heat flux at metal/mould interface during casting solidification', *Int. J. Cast Met. Res.*, 2006, **19**, (3), 188–194.
2. Y. Hebi, Y. Man and F. Dacheng: '3-D inverse problem continuous model for thermal behavior of mould process based on the temperature measurements in plant trial', *ISIJ Int.*, 2006, **46**, (4), 539–545.
3. J. Brimacombe: 'Design of continuous casting machines based o heat-flow analysis: state-of-the-art review', *Can. Metall. Q.*, 1976, **15**, (2), 17–28.
4. D. Spuy, I, Craig and P. Pistorious: 'An optimization procedure for the secondary cooling zone of a continuous billet caster', *J. S. Afr. Inst. Min. Metall.*, 1999, **99**, 49–54.
5. B. Petrus, K. Zheng, X. Zhou, B. G. Thomas and J. Bentsman: 'Real-time, model-based spray-cooling control system for steel continuous casting', *Metall. Mater. Trans. B*, 2011, **42B**, 87–103.
6. S. Choudhary, D. Mazumdar and A. Ghosh: 'Mathematical modelling of heat transfer phenomena in continuous casting of steel', *ISIJ Int.*, 1993, **33**, (7), 764–774.
7. J. Ma, Z. Xie and G. Jia: 'Applying of real-time heat transfer and solidification model on the dynamic control system of billet continuous casting', *ISIJ Int.*, 2008, **48**, (12), 1722–1727.
8. F. Calzolari, I. Craig and P. Pistorious: 'Specification framework for control of the secondary cooling zone in continuous casting', *ISIJ Int.*, 1998, **38**, (5), 447–453.
9. R. Mahapatra, J. Brimacombe, I. Samarasekera, N. Walker, E. Paterson and J. Young: 'Mold behavior and its influence on quality in the continuous casting of steel slabs. Part I: industrial trials, mold temperature measurements, and mathematical moldeling', *Metall. Trans. B*, 1991, **22B**, 861.

10. S. Kumar, J. Meech, I. Samarasekera, J. Brimacombe and V. Rakocevik: 'Development of intelligent mould for online detection of defects in steel billets', *Ironmaking Steelmaking*, 1999, **26**, 269.
11. A. Paul, N. Pradhan, A. Ray, P. Bhor and S. Mazumdar: 'Assessment of heat extraction through slab caster mould', *Scand. J. Metall.*, 2000, **29**, 139–145.
12. L. Guo, X. Wang, H. Zhan, M. Yao and D. Fang: 'Mould heat transfer in the continuous casting of round billet', *ISIJ Int.*, 2007, **47**, 1108.
13. H. Gilles: 'Primary and secondary cooling control', in 'Making, shaping and treating of steel', Vol. 18, 1–52; 2003, Pittsburgh, PA, AISE Steel Foundation.
14. S. Summerfield and D. Fraser: 'A new heat transfer correlation for impinging zone heat transfer on a hot steel plate', *Can. Metall. Q.*, 2006, **45**, 69.
15. I. Samarasekera and C. Chow: 'Continuous casting of steel billets', in 'Making, shaping and treating of steel', Vol. 17, 1–46; 2003, Pittsburgh, PA, AISE Steel Foundation.
16. V. D. Tutarova, D. Safonov and N. Shapovalov: 'Density distribution of spray from flat spray nozzles in the secondary-cooling zone of a continuous caster', *Metallurgist*, 2012, **56**, 438–456.
17. J. Brimacombe, I. Samarasekera and J. Lait: 'Heat flow, solidification and crack formation', *Contin. Cast.*, 1984, **2**, 1–8.
18. K. Zheng, B. Petrus, B. Thomas and J. Bentsman: 'Design and implementation of a real-time spray cooling control system for continuous casting of thin steel slabs', Proc. AISTech Steelmaking Conf., Indianapolis, IN, USA, May 2007, AIST, Vol. 1, 1-15.
19. Y. Meng and B. Thomas: 'Heat transfer and solidification model of continuous slab casting: CON1D', *Metall. Mater. Trans. B*, 2003, **34B**, 685.
20. H. Wang, G. Li, Y. Lei, Y. Zhao, Q. Dai and J. Wang: 'Mathematical heat transfer model research for the improvement of continuous casting temperature', *ISIJ Int.*, 2005, **45**, 1291.
21. S. V. Patankar: 'Numerical heat transfer and fluid flow'; 1980, Washington, DC, Taylor & Francis.
22. M. Flemings: 'Solidification processing'; 1974, New York, McGraw-Hill.
23. J. Brimacombe: 'Design of continuous casting machine based on heat-flow analysis: state-of-the-art review', *Can. Metall. Q.*, 1976, **15**, 17–28.
24. J. Brimacombe and L. Baptista: 'Spray cooling in the continuous casting of steel', *Contin. Cast.*, 1984, **1**, 109–123.
25. X. Huang, B. Thomas and F. Najjar: 'Modeling of steel grade transition in continuous slab casting processes', *Metall. Trans. B*, 1992, **23B**, 379–393.
26. A. Howe: 'Estimation of liquidus temperature for steels', *Ironmaking Steelmaking*, 1988, **15**, 134–142.
27. H. Wang, G. Li, Y. Lei, Y. Zhao, Q. Dai and J. Wang: *ISIJ Int.*, 2005, **45**, 1291.
28. J. Brimacombe, F. Weinberg and E. Hawbolt: 'Heat flow, solidification and crack formation', *Contin. Cast.*, 1984, **2**, 215.
29. P, Ingerslev and H. Henein: 'An integral boundary approach for 1- and 2-D modeling of ingot reheating and cooling', *Iron Steelmaker*, 1997, **24**, 75–85
30. H. Muller and R. Jeschar: 'Investigation of heat transfer in a simulated secondary cooling zone in the continuous casting process', *Arch. Eisenhuttenwesen*, 1973, **44**, 589–594.
31. S. Hibbins: 'Characterization of heat transfer in the secondary cooling of a continuous slab', MSc thesis, University of British Columbia, Vancouver, BC, Canada, 1982.
32. J. Brimacombe, P. Agarwal, S. Hibbins, B. Prabhaker and L. Baptista: 'Heat flow, solidification and crack formation', *Contin. Cast.*, 1984, **2**, 109.